

Formation of Droplets and Mixing in Multiphase Microfluidics at Low Values of the Reynolds and the Capillary Numbers

Joshua D. Tice, Helen Song, Adam D. Lyon, and Rustem F. Ismagilov*

Department of Chemistry, The University of Chicago, 5735 South Ellis Avenue, Chicago, Illinois 60637

Received March 4, 2003. In Final Form: June 11, 2003

This paper reports an experimental characterization of a simple method for rapid formation of droplets, or plugs, of multiple aqueous reagents without bringing reagents into contact prior to mixing. Droplet-based microfluidics offers a simple method of achieving rapid mixing and transport with no dispersion. In addition, this paper shows that organic dyes at high concentrations should not be used for the visualization of flow patterns and mixing of aqueous plugs in multiphase flows in this system (fluorinated carrier fluid and PDMS microchannels). It reports an inorganic dye that can be used instead. This work focuses on mixing in plugs moving through straight channels. It demonstrates that, when traveling through straight microchannels, mixing within plugs by steady recirculating flow is highly sensitive to the initial distribution of the aqueous reagents established by the eddy flow at the tip of the forming plug (twirling). The results also show how plugs with proper distribution of the aqueous reagents could be formed in order to achieve optimal mixing of the reagents in this system.

Introduction

This paper characterizes a method of using flow of immiscible fluids in microfluidic channels to form plugs containing multiple aqueous reagents, mix these reagents inside the plugs under optimal conditions in straight channels, and then reliably transport them through the channels. We define plugs as droplets that block the channel but do not wet the walls. This method solves two problems of microfluidics—mixing and dispersion. In the preliminary studies reported recently,¹ we have shown that droplet-based microfluidics can be successfully used to measure the rate of a chemical reaction on a millisecond time scale.

Dispersion of the solutes along the length of microfluidic channels is a problem associated with pressure-driven laminar flow; it is known as Taylor dispersion.² Dispersion leads to dilution of the samples injected into the microchannels, leads to cross-contamination of the samples, and limits the throughput of a microfluidic system. Some dispersion occurs due to flow—the pressure-driven flow profile is parabolic, with the fluid in the center of the capillary moving at a higher velocity than the fluid near the walls. Additional dispersion also occurs due to diffusion; even in the absence of flow, molecules are free to diffuse along the length of the channel. The dispersion due to flow can be removed by the use of electroosmotic flow (EOF), which has a flat flow profile,³ although there is still some dispersion around bends of microchannels. EOF has been used very effectively for DNA separations.^{4,5} However, EOF is not sufficiently robust for many ap-

plications: it requires high voltages, and it is highly sensitive to contaminations of the charged surfaces used to drive the flow. In addition, only low flow rates can be achieved using EOF.

The simplest solution to the dispersion problem is to localize the reagents within droplets surrounded by an immiscible fluid. Reagents no longer disperse along the whole length of the channel; rather dispersion is confined to the volume of the plug. A similar approach has been used for many years in biochemical blood analyzers,⁶ although, in the case of analyzers, the stream of the aqueous reagent fluid wets the walls of the glass capillary and nonwetting air bubbles are used to segment the reagent fluid. The droplets have been successfully used to localize reagents in microfluidics.^{4,7–11} An elegant droplet metering system has been used in a DNA analyzer.⁴

Mixing is the second problem associated with the laminar flow. Two streams injected into a channel at low Reynolds number², Re , flow laminar side-by-side, with mixing only by diffusion.^{2,12,13} Rapid mixing of chemical reagents in microchannels is difficult to achieve, and a significant research effort has been devoted to solving this problem.^{14–17} Hydrodynamic focusing,^{18,19} injecting streams of reagents into a common channel as multiple lamina,²⁰ chaotic advection at intermediate²¹ and low^{16,17} values of Re , and the use of beads in microchannels²² are some of the methods developed to enhance mixing. These methods do not eliminate dispersion, although chaotic advection has been shown to reduce it significantly.^{16,17}

* Corresponding author.

(1) Song, H.; Tice, J. D.; Ismagilov, R. F. *Angew. Chem., Int. Ed.* **2002**, *42*, 768–772.

(2) Bird, R. B.; Stewart, W. E.; Lightfoot, E. N. *Transport Phenomena*; Wiley: New York, 2002.

(3) Medintz, I. L.; Paegel, B. M.; Blazej, R. G.; Emrich, C. A.; Berti, L.; Scherer, J. R.; Mathies, R. A. *Electrophoresis* **2001**, *22*, 3845–3856.

(4) Burns, M. A.; Johnson, B. N.; Brahma, S. N.; Handique, K.; Webster, J. R.; Krishnan, M.; Sammarco, T.; Man, P. M.; Jones, D.; Heldinger, D.; Mastrangelo, C. H.; Burke, D. T. *Science* **1998**, *282*, 484–487.

(5) Chou, H.-P.; Spence, C.; Scherer, A.; Quake, S. *Proc. Natl. Acad. Sci. U.S.A.* **1999**, *96*, 11–13.

(6) Snyder, L.; Levine, J.; Stoy, R.; Conetta, A. *Anal. Chem.* **1976**, *48*, 942.

(7) Burns, M. A. *Science* **2002**, *296*, 1818–1819.

(8) Fu, A. Y.; Spence, C.; Scherer, A.; Arnold, F. H.; Quake, S. R. *Nat. Biotechnol.* **1999**, *17*, 1109–1111.

(9) Cho, S. K.; Moon, H.; Fowler, J.; Kim, C. J. *Proc. ASME IMECE* **2001**, 1–7.

(10) Fowler, J.; Moon, H.; Kim, C. J. *Proc. 15th IEEE Conf. MEMS* **2002**, 97–100.

(11) Taniguchi, T.; Torii, T.; Higuchi, T. *Lab Chip* **2002**, *2*, 19–23.

(12) Kamholz, A. E.; Yager, P. *Sens. Actuator, B: Chem.* **2002**, *82*, 117–121.

(13) Ismagilov, R. F.; Stroock, A. D.; Kenis, P. J. A.; Whitesides, G.; Stone, H. A. *Appl. Phys. Lett.* **2000**, *76*, 2376–2378.

All methods of mixing attempt to reduce the striation length, stl (m), the distance over which mixing can occur by diffusion. For diffusion in one dimension the mixing time, t_{mix} (s), is given by

$$t_{\text{mix}} = stl^2/2D \quad (1)$$

where D (m^2/s) is the diffusion constant. For a protein with a diffusion constant of $D = 10^{-10} \text{ m}^2/\text{s}$, reducing stl from 100 to 1 μm reduces t_{mix} from 50 s to 5 ms. A droplet moving through a channel develops recirculating flow, that enhances mixing by reducing the striation length.²³ Our preliminary results¹ indicated that mixing in moving plugs can be as fast as a few milliseconds. Thus, droplet-based microfluidics is attractive because it has the potential to solve both the mixing and dispersion problems.

This paper describes how we (i) experimentally characterized a simple method¹ for rapid formation of plugs of multiple reagents without bringing reagents into prior contact, (ii) designed a set of dyes useful for visualization of flow patterns inside aqueous plugs, (iii) determined that, in straight microchannels, mixing within plugs by the steady recirculating flow is highly sensitive to the initial distribution of the reagents, and (iv) established how plugs with proper distribution of the reagents can be formed in order to achieve rapid mixing in straight microchannels.

Experimental Section

Networks of microchannels with rectangular cross-sections were fabricated using rapid prototyping in poly(dimethylsiloxane) (PDMS).^{24–26} The PDMS used was Dow Corning Sylgard Brand 184 Silicone Elastomer, and devices were sealed using a Plasma Prep II (SPI Supplies). The surfaces of the devices were rendered hydrophobic by baking the devices at 120 °C for 2–4 h.

In Figure 2, the red aqueous streams were McCormick red food coloring (water, propylene glycol, FD&C Reds 40 and 3, propylparaben), the green aqueous streams were McCormick green food coloring (water, propylene glycol, FD&C yellow 5, FD&C blue 1, propylparaben) diluted 1:1 with water, and the colorless streams were water. In all other figures, red aqueous streams were $\text{Fe}(\text{SCN})_x^{(3-x)+}$ complexes prepared by mixing 0.067 M $\text{Fe}(\text{NO}_3)_3$ with 0.2 M KSCN. All remaining colorless aqueous streams were 0.2 M KNO_3 . PFD used was a 10:1 mixture of perfluorodecalin (mixture of cis and trans, 95%, Acros Organics) and 1*H*,1*H*,2*H*,2*H*-perfluorooctanol (Acros Organics).

Aqueous solutions were pumped using 100 μL Hamilton Gastight syringes (1700 series, TLL) or 50 μL SGE gastight

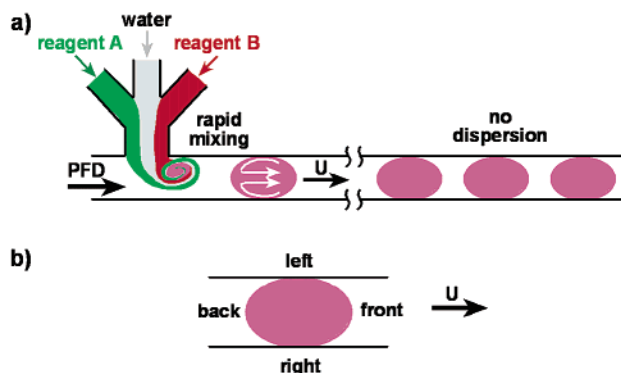


Figure 1. (a) Schematic illustration of the approach characterized in this paper to forming plugs of multiple aqueous solutions by injecting them into a stream of water-immiscible fluorinated fluid, PFD. Droplets were mixed rapidly by recirculation shown by white arrows. Plugs (droplets that block the channel but do not wet the walls) were transported with no dispersion. (b) Notation used throughout the paper to identify different regions of the plugs, relative to the direction of motion.

syringes. PFD was pumped using 1 mL Hamilton Gastight syringes (1700 series, TLL). The syringes were attached to microfluidic devices by means of Hamilton teflon needles (30 gauge, 1 hub). Syringe pumps from Harvard Apparatus (PHD 2000 Infusion pumps; specially ordered bronze bushings were attached to the driving mechanism to stabilize pumping) were used to infuse the aqueous solutions and PFD.

Microphotographs were taken with a Leica MZ12.5 stereomicroscope and a SPOT Insight Color digital camera (model #3.2.0, Diagnostic Instruments, Inc.). SPOT Advanced software (version 3.4.0 for Windows) was used to collect the images. Lighting was provided from a Machine Vision Strobe X-Strobe X1200 (20 Hz, 12 μF , 600 V, Perkin-Elmer Optoelectronics). To obtain an image, the shutter of the camera was opened for 1 s and the strobe light was flashed once with the duration of the flash being $\sim 10 \mu\text{s}$.

Images were analyzed using NIH Image software, Image J. Image J was used to measure periods and lengths of plugs from microphotographs such as those shown in Figure 7b. Periods corresponded to the distance from the center of one plug to the center of an adjacent plug, and the length of a plug was the distance from the extreme front to the extreme back of the plug (see Figure 1b for definitions of front and back).

Surface tensions were measured using the hanging drop method. A small ($\sim 1 \mu\text{L}$) drop of the fluorinated fluid was extruded into $\sim 1 \text{ mL}$ of the aqueous solution inside a disposable optical cell. A microphotograph of the drop was taken with a CCD camera equipped with a zoom objective. The shape of the drop, determined by the balance of gravity and surface tension, was analyzed as described previously.^{27–29}

To make measurements of the optical intensity of $\text{Fe}(\text{SCN})_x^{(3-x)+}$ complexes in plugs, microphotographs were saved in CMYK color mode in Adobe Photoshop 6.0. Using the same program, the yellow color channels of the microphotographs were then isolated and converted to gray scale images, and the intensities of the gray scale images were inverted. The yellow color channel was chosen to reduce the intensity of bright reflections at the extremities of the plugs and at the interface between the plugs and the channel. Following the work done in Photoshop, regions of plugs containing high concentrations of $\text{Fe}(\text{SCN})_x^{(3-x)+}$ complexes appeared white while regions of low concentration appeared black. Using Image J, the intensity was measured across a thin, rectangular region of the plug, located halfway between the front and back of the plug (white dashed lines in Figure 7a). The camera used to take the microphotographs of the system was not capable of making linear measurements of optical density. Therefore, our measurements of intensity were not quantitative. Several of the plots in

(14) Auroux, P.-A.; Iossifidis, D.; Reyes, D. R.; Manz, A. *Anal. Chem.* **2002**, *74*, 2623–2636.

(15) Auroux, P.-A.; Iossifidis, D.; Reyes, D. R.; Manz, A. *Anal. Chem.* **2002**, *74*, 2637–2652.

(16) Stroock, A. D.; Dertinger, S. K.; Whitesides, G. M.; Ajdari, A. *Anal. Chem.* **2002**, *74*, 5306–5312.

(17) Stroock, A. D.; Dertinger, S. K. W.; Ajdari, A.; Mezic, I.; Stone, H. A.; Whitesides, G. M. *Science* **2002**, *295*, 647–651.

(18) Knight, J. B.; Vishwanath, A.; Brody, J. P.; Austin, R. H. *Phys. Rev. Lett.* **1998**, *80*, 3863–3866.

(19) Pabst, S. A.; Hagen, S. J. *Biophys. J.* **2002**, *83*, 2872–2878.

(20) Bessoth, F. G.; deMello, A. J.; Manz, A. *Anal. Commun.* **1999**, *36*, 213–215.

(21) Liu, R. H.; Stremmer, M. A.; Sharp, K. V.; Olsen, M. G.; Santiago, J. G.; Adrian, R. J.; Aref, H.; Beebe, D. J. *J. Microelectromech. Syst.* **2000**, *9*, 190–197.

(22) Seong, G. H.; Crooks, R. M. *J. Am. Chem. Soc.* **2002**, *124*, 13360–13361.

(23) Handique, K.; Burns, M. A. *J. Micromech. Microeng.* **2001**, *11*, 548–554.

(24) McDonald, J. C.; Whitesides, G. M. *Acc. Chem. Res.* **2002**, *35*, 491–499.

(25) McDonald, J. C.; Duffy, D. C.; Anderson, J. R.; Chiu, D. T.; Wu, H. K.; Schueller, O. J. A.; Whitesides, G. M. *Electrophoresis* **2000**, *21*, 27–40.

(26) Duffy, D. C.; McDonald, J. C.; Schueller, O. J. A.; Whitesides, G. M. *Anal. Chem.* **1998**, *70*, 4974–4984.

(27) Hansen, F. K. *J. Colloid Interface Sci.* **1993**, *160*, 209–217.

(28) Hansen, F. K.; Rodsrud, G. *J. Colloid Interface Sci.* **1991**, *141*, 1–9.

(29) Neumann, A. W.; Spelt, J. K. *Applied Surface Thermodynamics*; Marcel Dekker: New York, 1995.

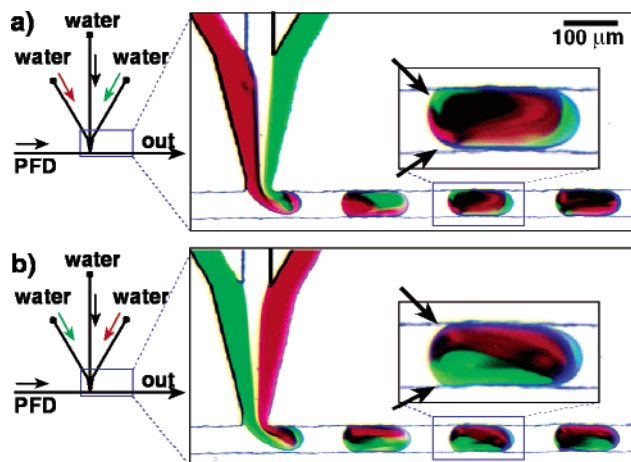


Figure 2. Concentrated solutions of organic dyes cannot be used to visualize true flow patterns and mixing inside plugs described in this paper because they perturbed the flow inside plugs. Left: Diagram of the microfluidic network. Right: Microphotographs of the plug-forming region of the microfluidic network. The colored aqueous streams were solutions of red and green food dyes. Plugs were traveling at 50 mm s^{-1} . The insets show enlarged microphotographs of plugs and their flow patterns. Arrows emphasize the difference in contact angles of the green and the red dyes with PDMS, indicating preferential wetting of the surface of the channels by the green dye.

the graphs of intensity versus relative position across the channel (Figure 7c) were shifted vertically by <50 units of intensity to adjust for nonuniform illumination of different parts of the images. These adjustments were justified because the shape of the distribution rather than absolute concentration was discussed in the paper.

Results and Discussion

Formation of a plug of multiple reagents¹ is schematically shown in Figure 1a. Two reagent streams were combined in a microchannel, separated by an inert stream. Since the flow was characterized by low values of the Re , the three streams remained laminar. The streams were continuously injected into a stream of flowing carrier fluid where they broke up into plugs transported by the carrier fluid. Microfluidic devices were fabricated using PDMS.^{24–26} We chose perfluorodecaline (PFD) as the water immiscible carrier fluid because fluorinated fluids, in contrast to hydrocarbon fluids, do not swell PDMS.

Visualization. We visualized flow patterns inside moving plugs by injecting marked streams of fluid into a plug and monitored the distribution of the marker as the plug proceeded through the channel. Marking streams in microchannels with absorption dyes requires high concentration of the dye, because thin microchannels provide only a short optical path. All organic dyes that we investigated, including the food dyes shown in Figure 2, affected the interfacial properties of aqueous solutions when dissolved at high concentrations. Therefore, visualizations made with these dyes were not representative of the flow patterns in plugs composed of dilute aqueous solutions.

By comparing Figure 2a and b, it becomes apparent that our food dyes did not act as inert markers in the aqueous phase (Figure 2). If the dyes acted as inert markers, one would expect that switching the inlets through which the red and green streams enter the plug-forming region would lead to the formation of plugs with complementary flow patterns (flow patterns with switched colors but otherwise identical). This is not what was observed (Figure 2)—the gross features of the flow patterns, and

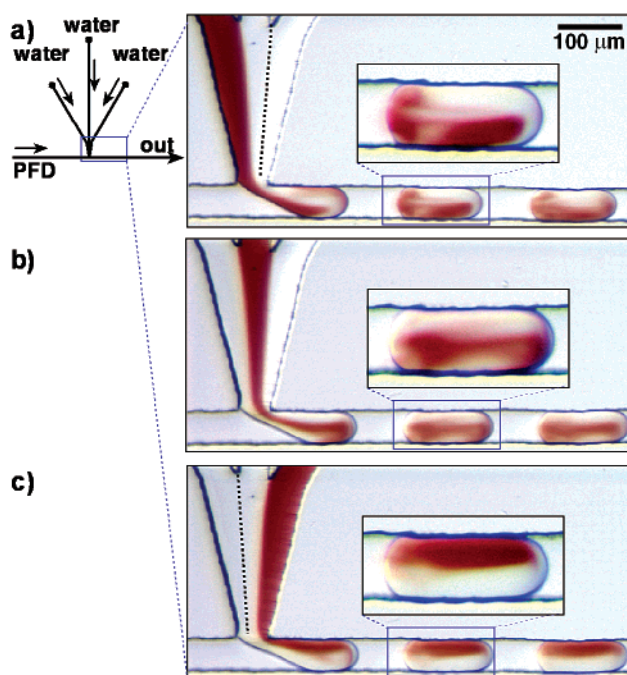


Figure 3. Aqueous solutions of $\text{Fe}(\text{SCN})_x^{(3-x)+}$ complexes and KNO_3 can be used to visualize flow patterns and mixing in plugs. Left: Diagram of the microfluidic network. Right: Microphotographs of the plug-forming region of the microfluidic network. The insets show enlarged microphotographs of plugs and their flow patterns. Changing the position of the dyed stream yielded plugs with complementary (switched) colored regions that were characteristic of the same flow pattern—for example, white areas in part a correspond to red areas in either part b or c. Plugs were traveling at 50 mm s^{-1} .

not just their colors, changed when the two streams were switched. The shape of the plugs also changed (black arrows in Figure 2). We have not characterized the details of the flow of food dyes in microchannels—a better-defined system where both the viscosity and interfacial tension can be varied independently would be required for a conclusive study. Nevertheless, these data were sufficient to conclude that organic dyes at high concentrations were unsuitable for visualization of flow patterns in aqueous plugs of multiphase flow in this system.

To observe flow patterns without perturbing the flow in aqueous plugs, we used a red aqueous solution of an inorganic complex $\text{Fe}(\text{SCN})_x^{(3-x)+}$ ($x \sim 3$, absorption maximum $\lambda_{\text{max}} \sim 480 \text{ nm}$, extinction coefficient $\epsilon \sim 5 \times 10^3 \text{ cm}^{-1} \text{ M}^{-1}$) prepared by mixing $0.067 \text{ M Fe}(\text{NO}_3)_3$ with 0.2 M KSCN (the viscosity of the solution of the complex was $1.08 \pm 0.05 \text{ mPa s}$). The two colorless aqueous streams were 0.2 M KNO_3 (viscosity $1.00 \pm 0.05 \text{ mPa s}$). Both $\text{Fe}(\text{SCN})_x^{(3-x)+}$ and KNO_3 solutions had interfacial tension with the fluorinated carrier fluid of $12\text{--}14 \text{ mN/m}$. These solutions did not perturb the flow patterns inside plugs (Figure 3). Switching the position of the colored stream leads to the formation of plugs with complementary distribution of the dye; for example, white areas in plugs shown in Figure 3a corresponded to dark areas in plugs shown in Figure 3b and c. Flow patterns within plugs were reproducible. At different flow rates, flow patterns were similar except for blurring by diffusion at lower flow rates, consistent with the low value of Re for these flows. We used these aqueous solutions in all subsequent experiments.

Formation of Plugs—Surface Tension and the Capillary Number. To obtain clean transport of the reagents, the carrier fluid must wet the walls of the

microchannels preferentially over the aqueous phase. If this condition is satisfied, the aqueous phase does not come in contact with the walls and remains separated from the walls by a thin layer of the carrier fluid;^{30,31} the plugs are stable and do not leave any residue behind as they are transported through the channels. To achieve this condition,²⁹ the surface tension at the water/PDMS interface (~ 38 mN/m)³² has to be higher than the surface tension at the water/PFD interface (~ 55 mN/m). We added 1*H*,1*H*,2*H*,2*H*-perfluorooctanol to PFD as a surfactant, which reduced the surface tension at the water/PFD interface. Using the hanging drop method,^{27–29} we measured the surface tension at the interface of water (or various aqueous buffers or solutions of $\text{Fe}(\text{SCN})_x^{(3-x)+}$ complexes) and the fluorinated 1*H*,1*H*,2*H*,2*H*-perfluorooctanol/PFD mixture to be 12–14 mN/m. In this paper we refer to this mixture of fluorinated fluids as carrier fluid or simply as PFD.

The surface tension at the water/PFD interface must be sufficiently high in order to avoid destruction of plugs by shear. Formation of plugs can be characterized by the dimensionless Capillary number, Ca ,

$$Ca = U\mu/\gamma \quad (2)$$

where U (m s^{-1}) is the velocity of the flow, γ (N m^{-1}) is the surface tension at the water/PFD interface, and μ ($\text{kg m}^{-1} \text{s}^{-1}$) is the viscosity of the fluid. U was determined by dividing the total volumetric flow rate by the cross-sectional area of the channel. The viscosity of PFD is $5.10 \times 10^{-3} \text{ N m}^{-1}$, and the viscosity of water is $1.00 \times 10^{-3} \text{ N m}^{-1}$. Water-in-oil droplets are commonly formed in microchannels.^{33–35} When shear is used at high values of Ca , the diameter of the droplets r (m) is then described by the equation^{33,36}

$$r \sim w\gamma/(\mu U) = w/Ca \quad (3)$$

where w (m) is the cross-sectional dimension of the channel and U/w is the shear rate (s^{-1}). At values of $Ca > 1$, droplets with the diameter smaller than the dimensions of the channel form. Under these conditions, the size of droplets linearly depends on the inverse of the flow velocity (eq 3), and droplets of various sizes form a range of interesting patterns.³³

We operated our system at low values of Ca ($< \sim 0.1$). Equation 3 did not predict the size of plugs in our system. The length of plugs was virtually independent of the total flow rate (Figure 4a and Figure 5) and of Ca . In addition, the period (p (m), the center-to-center distance between adjacent plugs) remained relatively constant as the flow rate (and Ca) was varied (Figure 4a). Assuming that the period is known, then the mass-conservation can be used to estimate the length of plugs l (m) from the “water fraction”, wf —the value of $V_w/(V_w + V_f)$, where V_w and V_f are the relative volumetric flow rates of water, V_w

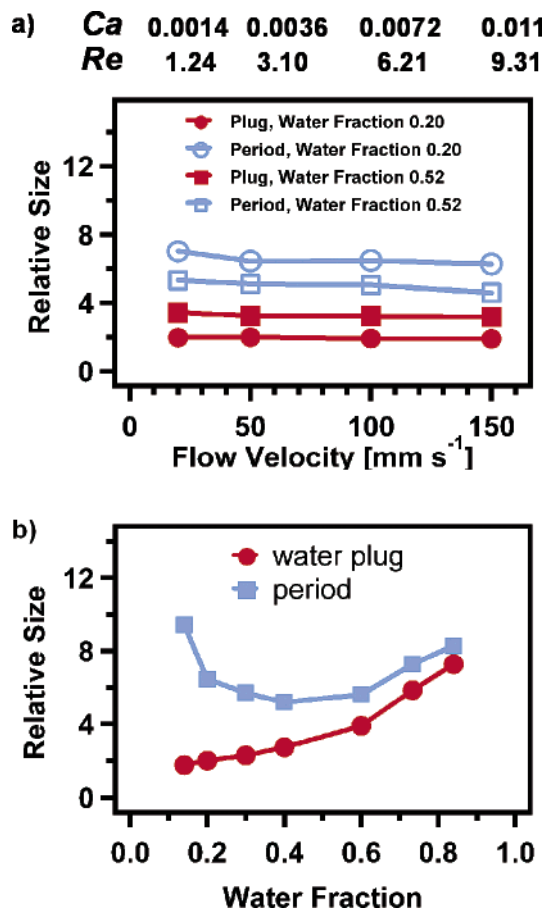


Figure 4. Data showing the spatial periods and the lengths of plugs as a function of (a) total flow velocity and (b) water fraction (defined in text). Values of Capillary (Ca) and Reynolds (Re) numbers are also shown. Plugs in part b are traveling at 50 mm s^{-1} . All measurements of length are reported relative to the width of channels ($50 \mu\text{m}$). Relative size is defined as the ratio of the length of the plug to the width of the channel.

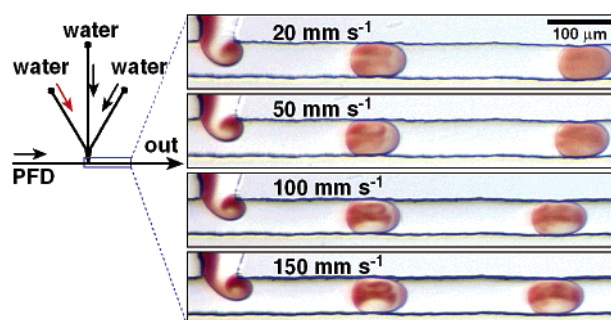


Figure 5. Microphotographs illustrating weak dependence of periods, length of plugs, and flow patterns inside plugs on total flow velocity. Left: Diagram of the microfluidic network. Right: Microphotographs of plugs formed at the same water fraction (0.20), but at different total flow velocities. The Capillary numbers were 0.0014, 0.0036, 0.0072, and 0.011, respectively, from top to bottom. The corresponding Reynolds numbers were 1.24, 3.10, 6.21, and 9.31.

($\mu\text{L}/\text{min}$), and the fluorinated fluid, V_f ($\mu\text{L}/\text{min}$) (eq 4).

$$l = pV_w/(V_w + V_f) = p \times wf \quad (4)$$

The length of plugs could be easily controlled by varying the relative volumetric flow rates of the aqueous and fluorine streams (Figure 4b). Short plugs formed when the flow rate of the aqueous stream was lower than that of the fluorine stream, and long plugs formed when the

(30) Bico, J.; Quere, D. *J. Fluid Mech.* **2002**, *467*, 101–127.

(31) Bico, J.; Quere, D. *J. Colloid Interface Sci.* **2002**, *247*, 162–166.

(32) Reiter, G.; Khanna, R.; Sharma, A. *Phys. Rev. Lett.* **2000**, *85*, 1432–1435.

(33) Thorsen, T.; Roberts, R. W.; Arnold, F. H.; Quake, S. R. *Phys. Rev. Lett.* **2001**, *86*, 4163–4166.

(34) Sugiyama, S.; Nakajima, M.; Seki, M. *Langmuir* **2002**, *18*, 5708–5712.

(35) Anna, S. L.; Bontoux, N.; Stone, H. A. *Appl. Phys. Lett.* **2003**, *82*, 364–366.

(36) Taylor, G. I. *Proc. R. Soc. London A* **1934**, *146*, 501–523.

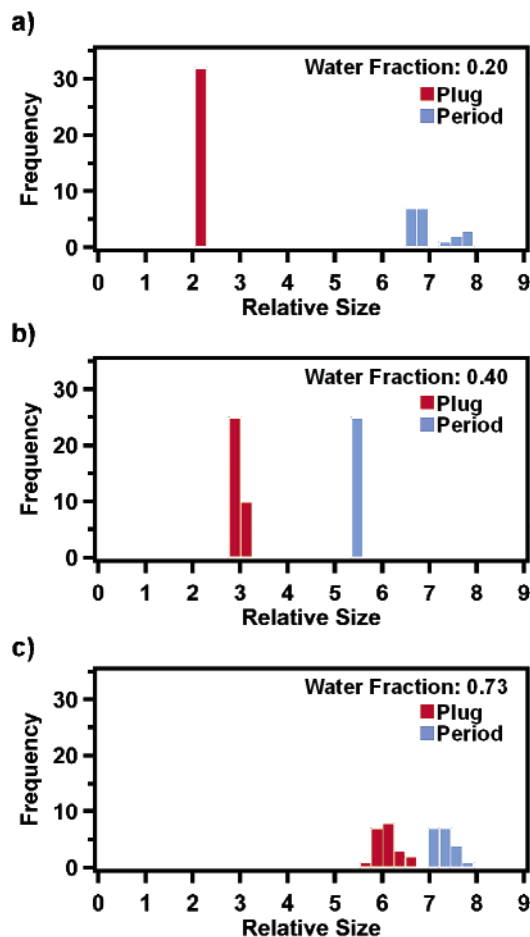


Figure 6. Histograms demonstrating the distribution of periods and lengths of plugs where the water fractions were (a) 0.20, (b) 0.40, and (c) 0.73. The total flow velocity was 50 mm s^{-1} , $Ca = 0.0036$, and $Re = 3.10$ in all cases. The period p (m) is the center-to-center distance between adjacent plugs. “Frequency” refers to the number of plugs or periods of a particular size in the histogram.

flow rate of the aqueous stream was higher than that of the fluoruous stream. The dependence of the length of the plugs on the water fraction deviates from the linearity suggested by eq 4 for two reasons: (i) This equation is approximate because it ignores the curvature at the sides of the plugs and assumes that plugs are parallelepipeds. This assumption predicts length that is too low for the small, almost spherical plugs. (ii) The period p itself depends on the water fraction. The period should become infinite at extreme values of $wf = 0$ and $wf = 1$. As water fraction was changed from ~ 0.15 to ~ 0.85 , the period varied by a factor of ~ 2 , passing through a minimum at the water fraction of ~ 0.50 (Figure 4b). This dependence of p introduced additional positive curvature to the graph of l versus wf in Figure 4b. Despite these deviations, the length of plugs l could be easily estimated.

Plugs of constant length could be formed reproducibly at intermediate values of water fraction, $0.20 < wf < 0.80$ (Figure 6). We have collected statistics describing the lengths of plugs l formed when water fraction was set to 0.20, 0.40, and 0.73. Irregular motion of the syringe pumps induced fluctuations in relative flow rates; therefore, fluctuations in period were observed (for these experiments, we used two separate syringe pumps for the fluoruous and aqueous phases). The fluctuations of flow rates affected the water fraction and became especially noticeable when the flow rates of the aqueous and the

fluoruous streams became significantly different (Figure 6a and c). The period was also more sensitive to changes in water fraction at extreme values of water fraction (Figure 4b). The length of plugs formed in flows driven by a syringe pump varied by about 3–20% of their length, depending on the water fraction. This level of monodispersity was adequate for the studies of mixing described below.

Mixing. Mixing in moving plugs occurs by recirculating flow (white arrows in Figure 1) caused by the shearing interactions of the fluid inside the plug with the stationary wall.³⁷ These closed recirculation flows are localized in the left and right halves of the plug (Figure 1). Theoretical studies by Burns²³ indicate that, for ideal initial conditions, the recirculating flow reduces the striation length, $stl(m)$:

$$stl(d) = stl(0) \times l/d \quad (5)$$

as a function of l/d , where d (m) is the distance traveled by the plug and l (m) is the length of the plug;²³ $stl(0)$ is the initial striation length in a plug, and $stl(d)$ is the striation length after a plug has traveled a distance d through the channel.

According to eq 5, reduction of stl by these steady flows depends on both d and l . One complete cycle of recirculation occurs when the plug has traveled its length, $d = l$. After d/l complete cycles of recirculation, the stl will have decreased inversely proportionately to the number of cycles. Therefore, eq 5 predicts that shorter plugs will mix in a shorter distance, d , and therefore in a shorter time, t_{mix} , at constant U . This prediction is certainly valid under ideal initial conditions.²³ In our system, the process of plug formation leads to a nonideal distribution of the solutions in the plug, and mixing may occur faster or much slower than predicted for the ideal initial conditions.

When the two solutions to be mixed are initially located in the front and back halves (defined in Figure 1b) of the plug, then recirculation effectively reduces the stl and this results in efficient mixing after several d/l cycles (Figure 7a1). However, if the two solutions are localized in the left and right halves (defined in Figure 1b) of the plug, then the stl is not affected by recirculating flows and therefore mixing is inefficient (Figure 7a2).

The initial distribution of the marker in the plug depended strongly on the details of plug formation. As the stationary aqueous plug was extruded into the flowing carrier fluid, shearing interactions between the flow of the carrier fluid and the aqueous phase induced an eddy that redistributed the solution of the marker to different regions of the plug. We refer to the formation of this eddy as “twirling”. Inertial effects did not induce twirling; twirling was present at both the low values of Re and the high values of Re , and it occurred at all flow velocities, although the flow pattern of this eddy was slightly affected by the velocity (Figure 5).

Twirling redistributed the marker by transferring it from the right to the left side of the plug (Figure 7b). Twirling was present during the formation of plugs of all lengths, but its importance for mixing depended on the length of the plug. Twirling occurred only at the tip of the forming plug before the tip made contact with the right (defined in Figure 1b) wall of the microchannel. The amount of twirling in a plug was related to the amount of the carrier fluid that flowed past the tip; this amount was significantly larger for short plugs than for long plugs

(37) This interaction may be modulated by the thin wetting layer of the carrier fluid separating the droplet from the wall, but this effect is small because the carrier fluid has slightly higher viscosity than the aqueous fluids.

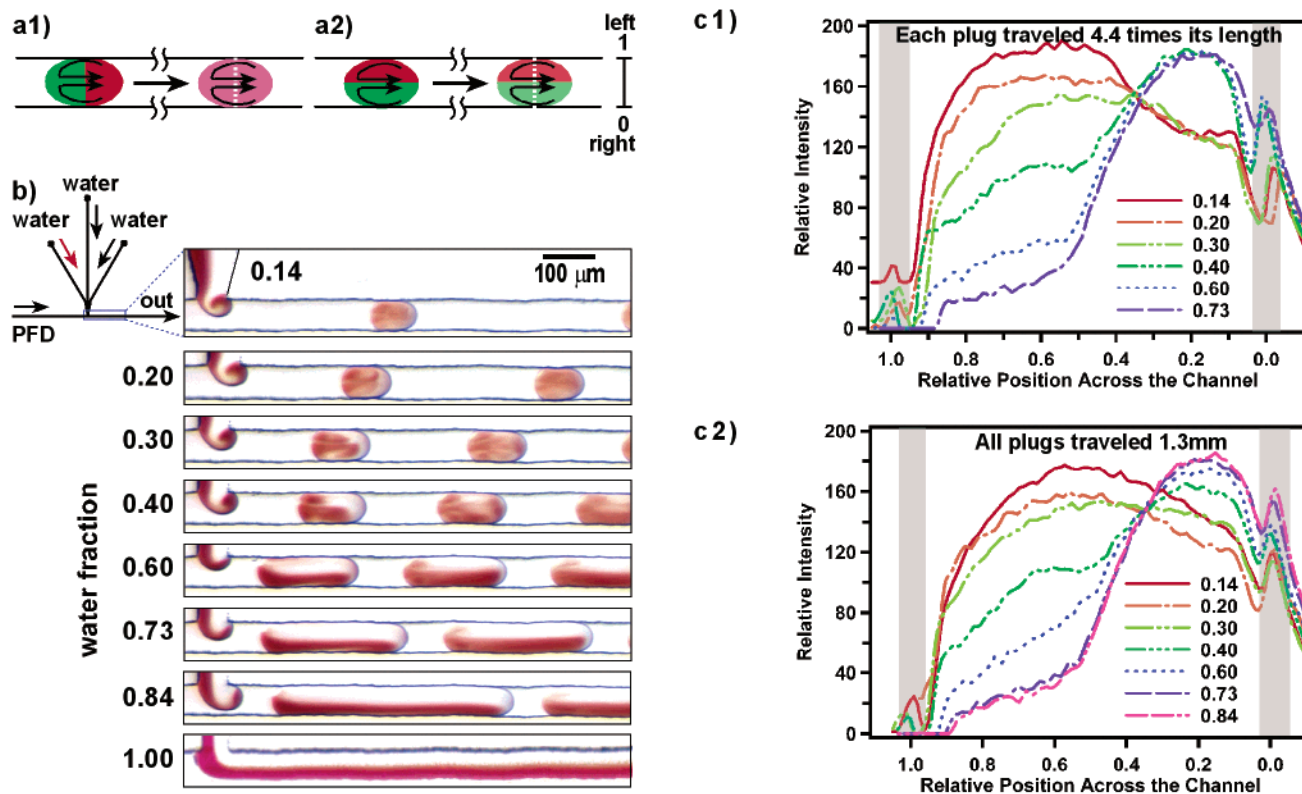


Figure 7. Effects of initial conditions on mixing by recirculating flow inside plugs moving through straight microchannels. (a1) Recirculating flow (shown by black arrows) efficiently mixed solutions of reagents that were initially localized in the front and back halves of the plug. Notations of front, back, left, and right are the same as those in Figure 1b. (a2) Recirculating flow (shown by black arrows) did not efficiently mix solutions of reagents that were initially localized in the left and right halves of the plug. (b) Left: Schematic diagram of the microfluidic network. Right: Microphotographs of different length plugs near the plug-forming region of the microfluidic network, for water fractions of 0.14–1.00. Plugs were traveling at 50 mm s^{-1} . (c1) A graph showing the relative optical intensity of $\text{Fe}(\text{SCN})_x^{(3-x)+}$ complexes in plugs of different lengths. Intensities were measured from left ($x = 1.0$) to right ($x = 0.0$) across the width of a plug (shown by white dashed lines in parts a1 and a2) after the plug had traveled 4.4 times its length through the straight microchannel. The gray shaded areas indicate the walls of the microchannel. (c2) Same as part c1, except each plug had traveled 1.3 mm. The d/l for each water fraction was 15.2 ($wf = 0.14$), 13.3 ($wf = 0.20$), 11.7 ($wf = 0.30$), 9.7 ($wf = 0.40$), 6.8 ($wf = 0.60$), 4.6 ($wf = 0.73$), and 2.7 ($wf = 0.84$).

(Figure 7b). Twirling affected only a small fraction of the long plugs and had a small effect on the distribution of the marker in these plugs (Figure 7b). Recirculating flow did not significantly accelerate mixing in longer plugs (Figure 7b, $wf = 0.73$) because not enough of the marker was transferred into the left side of the plug—the initial conditions for mixing in large plugs were similar to those shown in Figure 7a2. Mixing in the longest plugs was similar to mixing in a laminar flow in the absence of PFD (Figure 7b, $wf = 1.00$). In contrast, twirling accelerated mixing for shorter plugs (Figure 7b, $wf = 0.30$). Here, twirling redistributed the marker just enough into the left side such that nearly ideal initial conditions were created, like those in Figure 7a1. Under these conditions, we observed that the initial striation length was reduced by the formation of a spiral flow pattern shown schematically in Figure 1a. However, for even shorter plugs, mixing was worse (Figure 7b, $wf = 0.14$ and $wf = 0.20$) due to “overtwirling”. In this case, too much of the marker was transferred into the left side of the plug. When overtwirling occurred, mixing was less efficient because initial conditions resembled those observed for longer plugs (Figure 7b, $wf = 0.40$), except that the red markers occupied the opposite side of the plug.

We have created two intensity plots (Figure 7c) that show the relative concentration of the marker within the plug across the channel at the different water fractions (Figure 7b). For these plots, the general shape of each curve can qualitatively identify which initial condition

results in the most efficient mixing. The most efficient mixing corresponds to a curve with minimal fluctuations in intensity (the marker is evenly distributed across the plug). To further investigate the effects of twirling on mixing, intensity was measured across each plug after it traveled a distance d of 4.4 times its length l (Figure 7c1). If twirling is ignored, under these conditions of constant d/l for all plugs, eq 5 predicts equivalent mixing in all plugs. Equation 5 is undoubtedly valid²³ for the ideal initial conditions (Figure 7a1), and deviations from the predictions of the equation can be safely attributed to the effect of twirling. For the longer plug with $wf = 0.73$ and $wf = 0.60$, the plugs were not well mixed: the relative intensity curve was much higher on the right side of the plug than on the left side of the plug. For the shorter plug with $wf = 0.30$, the mixing curve was fairly smooth and so the plug was well mixed. For $wf = 0.30$, we estimated mixing time $\sim 25 \text{ ms}$ under these conditions. Mixing time could be reduced further by increasing the flow rate, but we have not been able to reach the $\sim 2 \text{ ms}$ mixing time observed for mixing by chaotic advection.¹ This fact is consistent with the lower mixing efficiency of steady recirculating flows rather than that of time-dependent flows.³⁸ For the shortest plugs with $wf = 0.14$, the relative intensity was higher on the left side of the plug, and

(38) Ottino, J. M. *The Kinematics of Mixing: Stretching, Chaos, and Transport*; Cambridge University Press: Cambridge, 1989.

therefore, this plug was overtwirled, in agreement with the images in Figure 7b.

The second graph (Figure 7c2) shows the intensity measured across each plug after it traveled a fixed distance, $d = 1.3$ mm. Except for the longest plug of $wf = 0.73$, all plugs have traveled a longer distance in the second graph than in the first graph. Therefore, in this second graph, more mixing took place and the intensity curves showed more uniform distribution of the marker, especially for short plugs. For the longer plugs, the intensity curves remained similar to those observed in Figure 7c1. Under these conditions, if twirling was ignored, one would have expected that the shortest plugs ($wf = 0.14$) with the highest d/l ratio would have mixed faster than medium plugs ($wf = 0.30$). However, this was not the case, and we still saw the effects of overtwirling. We concluded that twirling was the most important factor in determining ideal conditions for mixing in plugs moving through straight microchannels.

Conclusions

In this paper, we have characterized experimentally a simple method for rapid formation of plugs of multiple reagents without bringing the reagents into prior contact. Plugs were formed at low values of the Capillary number and at low values of the Reynolds number, and therefore, the length of plugs and the flow patterns within them were only weakly dependent on the flow velocity. In addition, we have shown that organic dyes at high concentrations should not be used for the visualization of flow patterns and mixing in these systems. We found that an inorganic complex with a high extinction coefficient may be used to visualize unperturbed flow patterns in multiphase fluid flow. We used these experimental results to establish that, in straight microfluidic channels, mixing by steady recirculating flow within plugs was sensitive to the initial distribution of the reagents, and we described how the process of formation of the plugs affected this initial distribution. To achieve optimal mixing of the reagents in straight microchannels, plugs with the proper initial distribution of the reagents could be formed simply by adjusting the relative flow rates of the aqueous and fluoruous streams to the experimentally determined optimal value. The following questions remain to be an-

swered: What are the factors that determine the period of the instability leading to the formation of plugs? Is mixing by chaotic advection in plugs¹ less dependent on the initial conditions and the length of plugs than the mixing by twirling described here? What is the range of viscosities and interfacial tensions of the solutions and the carrier fluids where these two methods of mixing are applicable? These questions will serve as the basis for future experimental and theoretical work and will complement current developments in multiphase microfluidics.^{39–42} We are beginning to use these systems as the basis of a microfluidic platform with rapid mixing and transport with no dispersion, useful for controlling chemical and biochemical systems on time scales from milliseconds to days. We are developing this platform for applications in rapid chemical synthesis and biochemical analysis, especially in proteomics.^{43–46}

Acknowledgment. This work was supported by the Camille and Henry Dreyfus New Faculty Award, the Research Innovation Award from Research Corporation, by Chicago MRSEC funded by NSF, and by the Predoctoral Training Grant (H.S.) of the NIH (GM 08720). This work has been performed at the Chicago MRSEC microfluidics facility. Photolithography was performed at MAL of UIC. We thank Professors Sidney R. Nagel and Thomas A. Witten for helpful discussions on the subjects of the Capillary number and the mechanisms of eddy formation.

LA030090W

(39) Ajmera, S. K.; Delattre, C.; Schmidt, M. A.; Jensen, K. F. *Sens. Actuator, B: Chem.* **2002**, *82*, 297–306.

(40) Losey, M. W.; Schmidt, M. A.; Jensen, K. F. *Ind. Eng. Chem. Res.* **2001**, *40*, 2555–2562.

(41) Zhao, B.; Viernes, N. O. L.; Moore, J. S.; Beebe, D. J. *J. Am. Chem. Soc.* **2002**, *124*, 5284–5285.

(42) Zhao, B.; Moore, J. S.; Beebe, D. J. *Science* **2001**, *291*, 1023–1026.

(43) Fields, S. *Science* **2001**, *291*, 1221.

(44) Ideker, T.; Thorsson, V.; Ranish, J. A.; Christmas, R.; Buhler, J.; Eng, J. K.; Bumgarner, R.; Goodlett, D. R.; Aebersold, R.; Hood, L. *Science* **2001**, *292*, 929–934.

(45) Lee, K. H. *Trends Biotechnol.* **2001**, *19*, 217–222.

(46) Zhou, Z. L.; Licklider, L. J.; Gygi, S. P.; Reed, R. *Nature* **2002**, *419*, 182–185.